4 Coal characterisation: conventional coal analyses

4.1 Introduction

An attempt to assess the process of devolatilization requires that the details of the parent coal characteristics be well understood. Fundamental coal properties such as rank, chemical structure and maceral composition play an important role in the characteristic- and kinetic behaviour of a coal during the devolatilization process. In this chapter the main aspects concerned with parent coal characterisation, with the aid of conventional analytical techniques, are presented and discussed. The following relevant sections are addressed:

- Choice and origin of coal samples and coal preparation (Section 4.2 and 4.3.);
- Overview of conventional coal characterisation analyses (Section 4.4.);
- Conventional coal characterisation techniques and apparatus (Section 4.5.);
- Characterisation results and discussion (Section 4.6.).

The different conventional characterisation techniques and results will be discussed under different sub-sections within the text.

4.2 Choice and origin of coal samples

Four coal samples were chosen on the basis of the following: (1) similar primary rank (bituminous), (2) varying vitrinite content between the coals, (3) relatively low ash content (preferably < 20 wt.% d.b.) and (4) difference in seam origin. The choice of the coals was done in consultation with both Mr. Johan de Korte from the CSIR and Bulletin 113 (Pinheiro, 1999). Three of the coals were selected from the Witbank Coalfield, which extends from Springs to Belfast in the East (Pinheiro, 1999). No. 2, 4 and 5 seam coals were chosen, where the No. 2

seam sample was obtained from Inyanda colliery (Exxaro), whilst the No. 4 and No. 5 seam samples were respectively obtained from Umlalazi colliery (Anglo Coal) and Greenside colliery (Anglo Coal). From a stratographical viewpoint, coal seams in the Witbank region are shallow, with most seams not exceeding a depth of 200 m (Cairncross, 2001). The thickness of the No. 2 seam ranges between 4.5 m and 20 m, whilst the thinner No. 4 seam (2.5m to 6.5 m) is split into different coal bands (4A, 4 Upper and 4 Lower) due to presence of mudstone and/or siltstone partings (Jeffrey, 2005). The shallower No. 5 seam can range in thickness to up to 2 m and is commonly used for metallurgical purposes (Jeffrey, 2005). The difference in depositional depth between seams No. 2 and No. 4 can range from 15 m to 50 m, whilst seam 5 has a depositional depth of between 20 m and 40 m higher than seam No. 4.

Furthermore the No. 2 seam has formed the backbone of the South African coal industry for over a century and is reaching its limit due to extensive mining. Currently, several collieries are employing open-cast techniques to recover this coal (Pinheiro, 1999). The No. 2 seam sample obtained from Exxaro's Inyanda mine is currently being sold for utilization as a steam coal (Exxaro, 2010; Jeffrey, 2005). In contrast however, the No. 4 seam is normally of poor quality, consisting of dull to dull lustrous coal, with the upper portion having the lowest quality. Mining is therefore restricted to the lower 3.5 m of this seam. Furthermore, this seam is generally used as a power station feedstock and for domestic steam applications (Jeffrey, 2005). The No. 5 seam coal obtained from Greenside colliery is mainly used as a blend coking coal and metallurgical coal (Jeffrey 2005; Smith & Whittaker, 1986).

The fourth coal was selected from the Soutpansberg Coalfields, which stretches over a distance of close to 300 km from the eastern border of the Kruger National Park to west of Alldays in the Limpopo province. The coal was obtained from Tshikondeni coal mine (Exxaro) in the Venda-Pafuri sector of the coalfield and is mainly used as a steam coal or coking coal (Exxaro, 2010; Pinheiro, 1999). The main seam of the Venda-Pafuri deposit is about 3.5 m thick and consists of several coal bands inter-layered with carbonaceous mudstone (Cairncross, 2001). Two seams are distinguishable (No. 1 and No. 2 seam), with the lowest seam approximately 72 m from the surface. Seam thickness varies from 0.55 m thick for No. 1 seam to 6 m total thickness for No. 2 seam (Jeffrey, 2005). For convenience, the coals will be henceforth referred to as: INY (No. 2 seam - Inyanda mine), UMZ (No. 4 seam - Umlalazi mine), G#5 (No. 5 seam - Greenside mine) and TSH (Tshikondeni mine) throughout the following chapters.

4.3 Coal preparation

Approximately 300 kg of coal (in the “small nut” product range) was received from each individual coal mine and sampled according to the correct standards from the respective coal mines. The run of mine (ROM) Tshikondeni coal sample was, however, screened within an average particle size range of 20 mm at the plant itself. The TSH sample was sent to Advanced Coal Technology (ACT) for dense medium separation with TBE to obtain a 1.5 $g.cm^{-3}$ density cut sample. This was done in order to obtain a similar product specification as obtained from the beneficiation section of the Tshikondeni mine (the ROM sample is crushed to -13 mm prior to beneficiation on the mine). The collected samples (INY, UMZ, G#5 and TSH) were henceforth air-dried on a groundsheet for 4 to 5 days to establish equilibrium with the surrounding atmosphere. After air-drying the samples, the cone & quartering technique (Holdich, 2002) was employed to obtain a representative sample of the 300 kg batch obtained for each coal.

The representative sample of each coal was preferentially crushed in a jaw crusher (Samuel Osborne (SA) LTD, Model: 66YROLL), hammer mill (Usborn Coalequip Engineering (PTY) LTD. Speed: 425 rpm. Size: 4x6 macro crusher. model no.: 46-126) and rotary mill (Wenman Williams & Co. (PTY) LTD. 503A) to obtain particle size ranges of -10 mm and -3 mm respectively. All the mills were cleaned properly with compressed air prior to use to avoid any contamination with previously crushed coals. A Fritch Analyzette (Type 03.5025, no.: 4822) sieve shaker with different sieves was used to screen the samples into finer size fractions to be used in the characterisation analyses. The screened samples were split into smaller representative samples by using a rotary riffler (SMC rotary sample splitter. 220 Hz. 50/1 A. serial no.: 09/01/005) and stored and bagged in Nampak heat-sealable bags under nitrogen. Additional preparation steps are discussed in the relevant sections.

4.4 Overview of coal characterisation analyses

4.4.1 Conventional analyses

Conventional analyses refer to conventional techniques such as proximate-, ultimate-, petrographic-, etc. analysis that were conducted to assess the characteristics of the parent

coals. A summary of the conventional analyses conducted on the four coals is given in Table 4.1. The Table also includes the laboratories that were responsible for the analyses.

Table 4.1 Conventional characterisation analyses performed on the four coal samples.

Characteristic property	*Analysis*	*Laboratory responsible*
Chemical & Mineralogical	Proximate	Advanced Coal Technology
	Ultimate	Advanced Coal Technology
	Total Sulphur	Advanced Coal Technology
	Calorific value	Advanced Coal Technology
	Fischer-tar	Advanced Coal Technology
	Ash (XRF)	Advanced Coal Technology
	Mineral (XRD)	XRD Analytical & Consulting
Petrographic	Maceral composition	Petrographics SA
	Vitrinite reflectance	Petrographics SA
	Carbon-mineral structure	Petrographics SA
Physical	BET adsorption (CO_2 & N_2)	North West University
	Mercury porosimetry	North West University
	Free swelling index (FSI)	Advanced Coal Technology
	Gieseler fluidity and Ruhr dilatometry	Advanced Coal Technology

A description of the standard methods used for the conventional analyses is provided in Appendix A.1

4.5 Characterisation techniques and apparatus

4.5.1 Conventional analyses

4.5.1.1 Chemical- and mineralogical analyses

Chemical- and mineralogical analyses were conducted in order to assess the fundamental chemical- and elemental composition that comprises the coal matrix. Fischer analysis was also

conducted in order to evaluate the speciation of volatile products during devolatilization. Coal samples with a particle size range of -3 mm were provided for the chemical analyses. The standard methods used during the chemical- and mineralogical analyses are provided in Table 4.2.

Table 4.2 Methods used for chemical-and mineralogical analyses of the four coal samples.

Analysis	*Standard Method*
Proximate analysis:	
➢ Inherent moisture;	SANS 5925:2007
➢ Volatile matter;	SABS ISO 562:1998
➢ Ash;	SABS ISO 1171:1997
➢ Fixed carbon.	By difference
Ultimate analysis	ISO 12902
Calorific value	SABS ISO 1928:1995
Total Sulphur (IR spectrometry)	ISO 19759: 2006
Fischer-tar	SANS 6073:1984
Ash analysis (XRF)	ASTM D4326

For the XRD analyses, coal samples with a particle size of -75 µm were used. The samples were dried overnight in a vacuum oven at 80℃ to remove any surface absorbed moisture. A back loading preparation method was used to prepare the samples prior to analysis. The diffraction of each sample was measured by a PANalytical X'Pert Pro powder diffractometer, with X'Celerator detector and variable divergence- and receiving slits with Fe filtered Co-Kα radiation. The different phases were identified with the help of the X'Pert Highscore plus software, whilst the Rietveld method (Autoquan Program) was applied in the estimation and quantification of the relative phase amounts (wt.%) (Verryn, 2010).

4.5.1.2 Petrographic analyses

Coal petrology is generally referred to as the microscopic examination of coals and the information obtained from this analytical technique can provide a deeper insight into the organic composition, maturity and carbon-mineral associations contained within coals (Du Cann, 2010). Coal samples with a particle size of -3 mm were selected for petrographic analyses.

The petrographical blocks used for the analysis were prepared and polished in accordance with the ISO 7404-2 (1985) standard by the SABS in Pretoria (ISO, 1985). After preparation, the sample blocks were subjected to vitrinite reflectance measurements to determine the rank of the coals, and maceral point-count analyses to determine the petrographic compositions. Vitrinite random reflectance measurements were conducted according to the ISO 7404-5 (1994) standard in order to establish the rank of the four coals (ISO, 1994b). 100 measurements were taken on the vitrinites of each coal sample. For maceral group identification, a 500 point-count technique was employed in accordance with the ISO 7404-3 (1994) standard (Du Cann, 2010; ISO, 1994a). The reactive inertinite macerals were identified and classified according to the method of Smith *et al.* (1983). In addition, total maceral reflectance scans were performed on each coal sample. A total of 250 readings were taken on all the macerals over the polished surface of each petrographical sample block (Du Cann, 2010; ISO, 1988). Coal microlithotype-, carbominerite-, and minerite analyses were carried out to investigate the organic-inorganic associations within the four coal samples. The latter was performed in accordance with the ISO 7404-4 (1988) standard. The general "freshness" or weathering index of the samples was also assessed (Du Cann, 2010).

4.5.1.3 Physical analyses

Mercury porosimetry

A Micromeritics AutoPore IV analyser was used to conduct mercury intrusion measurements on all four coals. Coal samples with an average particle size of 10 mm were used for the analyses. The samples were dried overnight in a vacuum oven at 80°C to remove any excess moisture from the external surface and pores. A penetrometer with a stem volume of 0.392 cm^3 (part no.: 942-61707-00) was used for all the intrusion experiments. For the high pressure intrusion measurements the samples were loaded to obtain a used stem volume of between 40% and 80%. Mercury was intruded at a contact angle of 130° while a surface tension of 0.0485 kPa.cm (485 $dyne.cm^{-1}$) was attained during the experiments. Low pressure analysis was conducted in order to determine the bulk density of the coals. The penetrometer containing the sample was connected to the low pressure port where it was evacuated to a pressure of 50 µmHg for 5 minutes, whereafter the mercury was introduced to a filling pressure of 3.59 kPa (0.52 psia). To determine structural related parameters such as the median pore radius, skeletal density and total porosity, high pressure mercury intrusion was conducted. For these measurements,

mercury was intruded at pressures ranging between 0.69 kPa and 413.7 MPa (0.1 to 60000 psia), while the corresponding intrusion volumes were measured (Bisset, 2005; Hattingh, 2009).

BET Adsorption

BET gas adsorption analyses were conducted on a Micromeritics ASAP 2010 Analyser on all four coal samples. This instrument is capable of determining pore sizes in the range of 4 Å to 5000 Å (Gregg & Sing, 1982; Stanley-Wood & Lines, 1992). Coal samples with an average particle size of 200 µm (-212+180 µm) were used for the adsorption analyses. The samples were dried overnight in a vacuum oven at 80℃ to remove any excess moisture from the external surface and pores. A sample mass of 0.2 g was loaded into the sample tube and connected to the degassing port of the analyser. In this port the sample was degassed for 48 hours at a temperature of 25℃ to a final pressure of 4 µmHg. Higher degassing temperatures were not used to prevent low temperature char formation (Hattingh, 2009). After degassing the samples, the sample tube was connected to the analysis port to start the appropriate adsorption analysis. Adsorption analyses were conducted with both CO_2 and N_2, respectively, as adsorbents. The short coal method, which includes measuring techniques such as: Langmuir, Dubinin-Radushkevich, Hovarth-Kawazoe, etc. was used for the CO_2 adsorption analyses (Hattingh, 2009). A similar degassing procedure to that for CO_2 adsorption analyses, was followed for N_2 BET, with the exception that the coal samples were degassed at 80℃ for 48 hours. This was done to ensure the removal of all water from the pores to prevent water freezing in the pores during the analyses. The Nitrogen Coal (pre-specified method at NWU) method was used for N_2 adsorption, which includes analyses such as: BET, Langmuir, Freundlich, Temkin, BJH etc. The analysis temperature for CO_2 adsorption was controlled at 273.15 K with ice, whilst liquid N_2 was used to control the temperature of the N_2 adsorption analyses at 77.35 K (Hattingh, 2009).

Plasticity measurements (FSI, Gieseler fluidity and Ruhr dilatometry)

Knowledge of coal plasticity and/or swelling behaviour required the evaluation of the FSI-, Gieseler fluidity- and Ruhr dilatometry of each coal, according to the SABS ISO 501(2003), SANS 6072 (2009) and ISO 10329 (2009) methods respectively.

4.6 Results and discussion

4.6.1 Conventional analyses

4.6.1.1 Chemical- and mineralogical analyses

Conventional analytical techniques such as proximate-, ultimate-, calorific value- and total sulphur analyses were performed on all four coals. The results obtained from these analyses are summarised in Table 4.3. All four coals were characterised as low ash yielding coals, with ash yields (SABS ISO 1171:1997) ranging between 13.5 wt.% and 18.6 wt.% (d.b.), thus confirming the coal choice criteria of Section 4.2. Furthermore, coal INY yielded the largest amount of ash with a value of 18.6 wt.% (d.b.), which can be explained by the fact that coal INY was obtained from the open-cast retrieving operation and not beneficiated. In terms of volatile matter it can be seen from Table 4.3 that the volatile matter content decreased in the order of G#5 > INY > UMZ > TSH from 34.1 wt.% (d.b.) to 20.5 wt.% (d.b.). It is, however, also important to notice that coal TSH contained the smallest amount of inherent moisture content, with a value of 0.7 wt.% (a.d.b.).

Calorific value is defined as the potential of a coal to generate heat during combustion (Koekemoer, 2009). The gross calorific values of all the coals were well above 25 $MJ.kg^{-1}$, with coal TSH having the largest value (29.7 MJ/kg d.b.). The higher calorific value of coal TSH can be attributed to its higher fixed carbon content (61.7 wt.% d.b.). According to the CKS 561-1982 standard, coals INY, UMZ, G#5 and TSH were graded on calorific basis as Grade C, Grade B, Grade A and Grade Sp coals, respectively. The significance of the CV grading system lies in the gross calorific value, where a Grade C coal contains a CV between 25.5 $MJ.kg^{-1}$ (a.d.b.) and 26.5 $MJ.kg^{-1}$ (a.d.b.), a Grade B coal contains a CV between 26.5 $MJ.kg^{-1}$ (a.d.b.) and 27.5 $MJ.kg^{-1}$ (a.d.b.), a Grade A coal contains a CV between 27.5 $MJ.kg^{-1}$ (a.d.b.) and 28.5 $MJ.kg^{-1}$ (a.d.b.), and a Grade Sp coal has a CV higher or equal to 28.5 $MJ.kg^{-1}$ (a.d.b.). In addition, coals TSH and G#5 can be respectively classified according to the American Society for Testing and Materials (ASTM) as low-volatile bituminous and high-volatile A bituminous coals (Smith *et al.*, 1994). The total sulphur contents of the four coals ranged between 0.70 wt.% (d.b.) and 1.71 wt.% (d.b.), with coal INY containing the largest amount of sulphur (organic + inorganic).

Table 4.3 Chemical analyses of the four coals.

			INY		*UMZ*		*G#5*		*TSH*	
			Air dry	***Dry basis***	***Air dry***	***Dry basis***	***Air dry***	***Dry basis***	***Air dry***	***Dry basis***
Proximate analysis	***Unit***	***Standard***								
Inherent moisture	wt.%	SANS 5925:2007	2.1	0.0	2.8	0.0	4.2	0.0	0.7	0.0
Ash	wt.%	SABS ISO 1171:1997	18.2	18.6	14.8	15.2	12.9	13.5	17.7	17.8
Volatiles matter (VM)	wt.%	SABS ISO 562:1998	25.0	25.5	24.5	25.2	32.7	34.1	20.4	20.5
Fixed Carbon (FC)	wt.%	By difference	54.7	55.9	57.9	59.6	50.2	52.4	61.3	61.7
TOTAL	wt.%		***100.0***	***100.0***	***100.0***	***100.0***	***100.0***	***100.0***	***100.1***	***100.0***
Fuel ratio (FC/VM)			2.2	-	2.4	-	1.5	-	3.0	-
Total Sulphur (IR Spectroscopy)	wt.%	ISO 19759	1.67	1.71	0.84	0.86	0.78	0.81	0.70	0.70
Gross Calorific Value (CV)	$MJ.kg^{-1}$	SABS ISO 1928:1995	26.3	26.9	26.9	27.7	27.6	28.4	29.5	29.7
Gross Calorific Value (CV) (a.f.b)	$MJ.kg^{-1}$		32.2	33.0	31.6	32.6	31.7	33.3	35.8	36.2
Grade (Based on CV, a.d.b.)	-	CKS 561-1982	Grade C		Grade B		Grade A		Grade Sp	
Ultimate analysis (Ash free basis)		ISO 12902								
Carbon	wt.%		79.1	81.2	81.1	83.8	75.4	79.2	90.1	90.8
Hydrogen	wt.%		4.6	4.7	4.2	4.3	5.2	5.5	4.9	5.0
Nitrogen	wt.%		2.0	2.0	2.0	2.1	2.1	2.3	2.1	2.1
Oxygen	wt.%	By difference	9.7	10.0	8.5	8.8	11.5	12.1	1.2	1.2
Total sulphur (IR Spectroscopy)	wt.%	ISO 19759	2.0	2.1	1.0	1.0	0.9	0.9	0.9	0.9
TOTAL	wt.%		***97.4***	***100.0***	***96.7***	***100.0***	***95.2***	***100.0***	***99.1***	***100.0***
C/H ratio	-		1.4	-	1.6	-	1.2	-	1.5	-
Atomic H/C ratio	-		0.69	-	0.62	-	0.83	-	0.66	-
Atomic O/C ratio	-		0.09	-	0.08	-	0.11	-	0.01	-

The total sulphur values of all the coals, except for coal INY, are well below or in the range of the authorised limit of between 0.8 wt.% and 1.0 wt.% (Milne, 2004; Thomas, 2002). The higher value of sulphur in INY can possibly be explained by the higher pyrite content of this coal due to the fact that no beneficiation was done on it. All four coals contained elevated levels of carbon, with TSH containing the largest amount with a significant value of 90.8 wt.% (d.a.f.). The high amounts of carbon in the coals make them ideal feed stocks for coal conversion processes such as gasification and combustion.

Oxygen content plays an important role in the prediction of the occurrence of active sites after devolatilization (Hashimoto *et al.*, 1986). From an oxygen point of view, coals INY, UMZ and G#5 contained very similar amounts, whereas coal TSH only contained about 1.2 wt.% (d.a.f.) of oxygen. Furthermore, no significant differences could be observed between the total H and -N contents of the four coals. The results obtained from the proximate- and ultimate analyses are in accordance with results published by De Jager (2002) and Pinheiro (1999).

In addition, Table 4.3 includes the values for the fuel ratio (FC/VM); and atomic H/C and -O/C ratios as calculated from the proximate- and ultimate analyses, respectively. With respect to the higher fuel ratio value (3.0) of coal TSH, it can be estimated that the energy obtained during coal conversion processes, such as gasification, will be the highest for this coal. No significant differences were observed between the H/C ratios, except for coal G#5 which had a slightly higher value. Coal TSH did, however, show a significantly lower O/C ratio (0.01), which suggests that this coal is highly aromatic in nature (Furimsky & Ripmeester, 1983).

A Fischer-assay was also performed on all four coals in order to assess the speciation of the volatile products of each coal during devolatilization. The results obtained from this analysis are provided in Table 4.4. From the results of the Fischer-assay it can be observed that tar yield increases in the order of UMZ < INY < TSH < G#5, with coal G#5 containing a substantial amount of 11.29 wt.% (a.f.b.) of tar. Gas production seems to be similar between the four coals, whilst a large difference is observed between the water yields of the four coals. The water yield from the Fischer-assay corresponds proportionally with what was observed with the inherent moisture content of the coals. Inversely, it can be seen that TSH contained the largest amount of coke/char (85.56 wt.% a.f.b.). Furthermore, a direct correlation (although not entirely linear) could be deduced between the oxygen content (d.a.f.) (Table 4.3.) and the Fischer-assay water

yield (Table 4.4.) of the four coals, suggesting that at least some of the water produced could be ascribed to the thermal decomposition of oxygen-containing structures within each coal.

Table 4.4 Fischer tar results for the four coals.

Analyses	*Unit*	*Standard*	*INY*	*UMZ*	*G#5*	*TSH*
Fischer tar analyses (a.f.b.)		SANS 6073:1984				
Coke/Char	wt.%		82.98	83.63	72.84	85.56
Tar	wt.%		6.69	5.80	11.29	7.62
Gas	wt.%		4.69	4.17	5.97	5.27
Water	wt.%		5.65	6.40	9.90	1.55
TOTAL	wt.%		***100.01***	***100.00***	***100.00***	***100.00***

The total amount of volatile matter (tar + gas) is however smaller than what was predicted with the proximate analysis. This can be explained by the fact that the Fischer-assay is normally performed at 520°C, while the volatile matter determination in the proximate analysis is determined at 900°C. Evaluating the distributions of mineral/inorganic constituents within coal required that XRD- and XRF techniques be applied. XRD was conducted on the raw coal samples, whereas XRF was done on the ash of the four samples. Ashing of the coal samples was performed by Advanced Coal Technology. The XRF analyses were conducted on a loss of ignition free basis (L.O.I.). The results obtained from these two techniques are provided in Table 4.5 and Table 4.6, respectively. The XRD results are only concerned with species in the crystalline phase and not the amorphous phase.

Chemical formulas for the different identified minerals are provided in Appendix A.2. It should be noted that some of the errors reported for the minor phase amounts are larger than the quantities obtained. This possibly entails the absence of those phases. The error obtained for the graphite could be over-estimated due to crystallite size effects. Furthermore, the term graphite refers to the carbon or organic component of the coals. Although not entirely correct, this term collectively refers to the organic part of the coal exhibiting a crystalline structure (Verryn, 2010). Apart from graphite, all four coals contained substantial amounts of kaolinite and quartz. Coals INY and UMZ, however, contained significantly less quartz (0.19 wt.% and 2.69 wt.%), but more calcite- and dolomite relative to G#5 and TSH. Negligible amounts of siderite

were observed in all the coals. Only a small amount of magnetite (0.35 wt.%) was observed in the INY coal.

Table 4.5 XRD (mineral analyses) results of all four coals.

Mineral species (Graphite basis)	*INY*		*UMZ*		*G#5*		*TSH*	
	wt.%	*Error (3σ)%*	*wt.%*	*Error (3σ)%*	*wt.%*	*Error (3σ)%*	*wt.%*	*Error (3σ)%*
Anatase	0.33	0.16	0.25	0.13	0.19	0.15	0.25	0.13
Calcite	***4.59***	***0.51***	***6.24***	***0.48***	***0.65***	***0.20***	***0.85***	***0.18***
Dolomite	***4.39***	***0.54***	***3.89***	***0.39***	***0.46***	***0.26***	***1.75***	***0.30***
Graphite	56.30	3.30	65.65	2.07	68.95	1.98	70.34	1.71
Kaolinite	***26.55***	***1.92***	***18.28***	***1.08***	***12.72***	***0.87***	***14.60***	***0.84***
Magnetite	0.35	0.19	0.00	0.00	0.00	0.00	0.00	0.00
Muscovite	2.33	0.66	0.79	0.39	3.21	0.66	3.52	0.54
Pyrite	4.74	0.39	1.66	0.16	2.53	0.21	0.56	0.12
Quartz	***0.19***	***0.14***	***2.69***	***0.33***	***11.15***	***0.75***	***7.81***	***0.51***
Rutile	0.16	0.12	0.10	0.10	0.14	0.20	0.10	0.11
Siderite	0.05	0.09	0.46	0.15	0.00	0.00	0.22	0.15
TOTAL	***100.00***		***100.00***		***100.00***		***100.00***	

Table 4.6 XRF (ash analyses-L.O.I. free basis) results on the ash of all four coals.

Ash species	*INY*	*UMZ*	*G#5*	*TSH*
	wt.% (d.b.)	*wt.% (d.b.)*	*wt.%(d.b.)*	*wt.% (d.b.)*
Al_2O_3	33.43	26.42	24.83	27.17
SiO_2	***39.00***	***37.91***	***63.14***	***59.30***
CaO	***9.04***	***18.83***	***1.87***	***3.01***
Cr_2O_3	0.03	0.03	0.03	0.01
Fe_2O_3	***7.75***	***5.97***	***5.32***	***3.30***
K_2O	0.55	0.55	1.28	1.51
MgO	1.76	1.51	1.07	0.99
MnO	0.06	0.11	0.02	0.03
Na_2O	N/D	N/D	0.15	0.65
P_2O_5	***0.78***	***2.42***	***0.77***	***0.41***
TiO_2	1.96	1.71	1.10	1.10
V_2O_5	0.03	0.03	0.02	0.02
ZrO_2	0.09	0.08	0.07	0.05
Ba	0.27	0.11	0.11	0.17
Sr	0.21	0.30	0.05	0.11
SO_3	***5.03***	***4.01***	***0.54***	***2.17***
TOTAL	***100.00***	***100.00***	***100.40***	***100.00***

The increased value of pyrite for INY tends to agree with the elevated elemental S levels from the ultimate analysis of this coal. From the evaluation of the species contained in the ash it is clear (Table 4.6) that all four coals are rich in Al_2O_3 and SiO_2, with coals G#5 and TSH containing significantly larger amounts of SiO_2 (63.14 wt.% and 59.3 wt.%, respectively). The large levels of these two species correspond to the large amount of clay- and quartz minerals (kaolinite and quartz) present in the samples (XRD analyses) (Spears, 2000). In addition, coal UMZ contained the largest amount of CaO (18.83 wt.%), followed by coal INY with a CaO content of 9.04 wt.%. This is mainly attributed to the large amounts of calcite and dolomite minerals present in these coals. Coal UMZ contained a relatively large amount of phosphate (P_2O_5) in comparison to the other coals, whilst both coals INY and UMZ also contained large amounts of SO_3.

4.6.1.2 Petrographic analyses

The results from the petrographic analyses are presented and discussed in the following text. The following aspects of petrology will be addressed:

- Reflectance measurements on both vitrinite and total macerals;
- Maceral (organic)- and microlithotype characteristics of each coal;
- Carbominerite- and minerite results;
- General condition of the analysed samples.

Reflectance measurements:

Reflectance analysis provides a suitable method for establishing the degree of maturity or rank of a particular coal (Du Cann, 2010). Vitrinite is chosen as the reference maceral for this purpose due to the fact that its reflectance increases uniformly as the coalification process progresses, thus making it a very reliable parameter which is independent of the content of vitrinite and the coal grade (Du Cann, 2010). The rank of some South African coals may prove to be anomalous during chemical determinations, mainly pertaining to the fact that South African coal is generally inertinite-rich.

In order to establish the rank of the four coals (INY, UMZ, G#5 and TSH), random reflectance measurements (in oil immersion) were conveniently taken on the vitrinite maceral Telovitrinite. The results obtained from these measurements are given in Figure 4.1 (reflectance histograms) and Table A.2. in Appendix A.3.

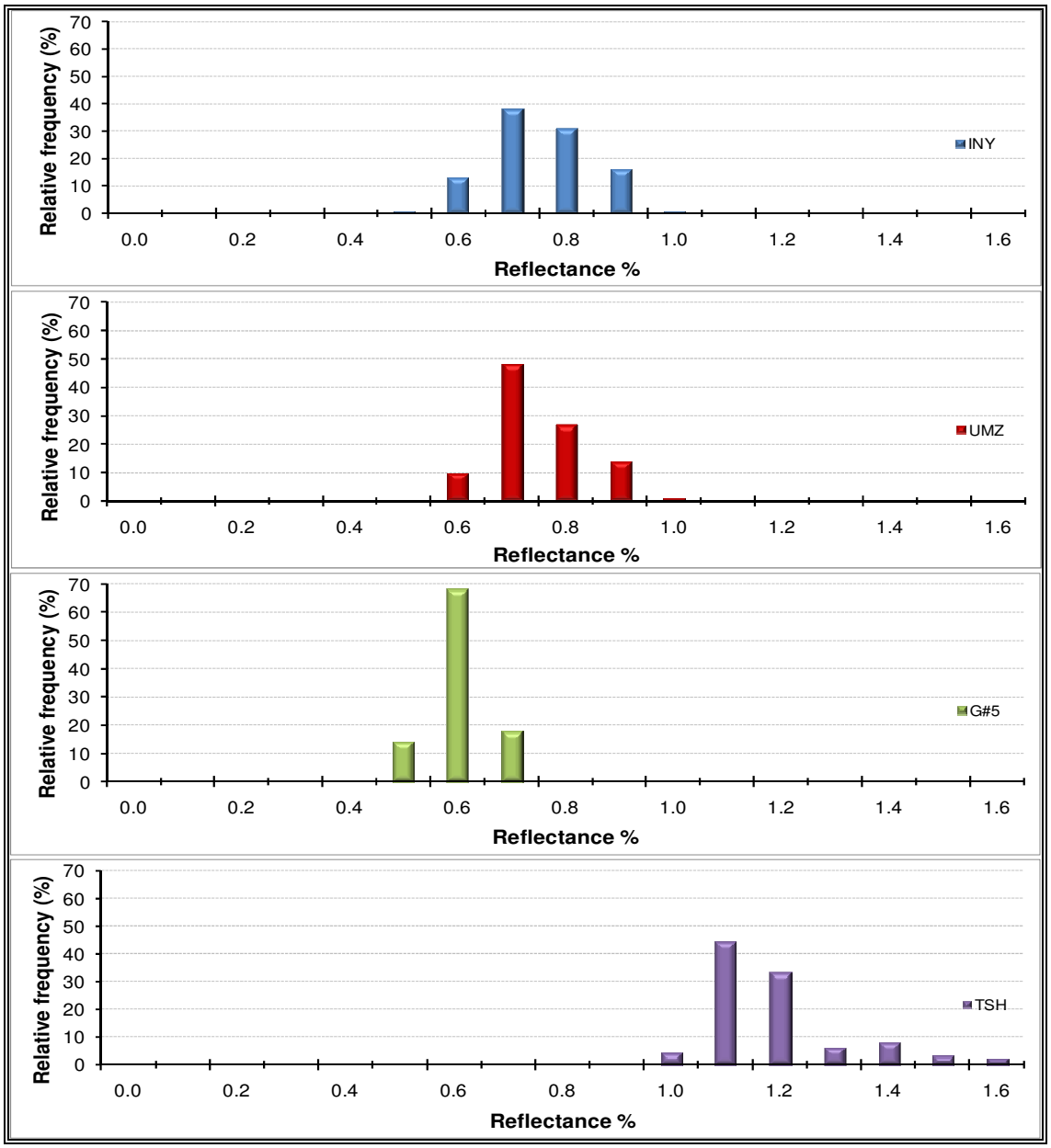

Figure 4.1 Vitrinite reflectance histograms of coals INY, UMZ, G#5 and TSH.

From Figure 4.1 it can be observed that the reflected vitrinites for coals INY, UMZ and G#5 typically occur in the 0.5% to 1.0% reflectance distribution range, whereas the reflectance

distribution for TSH falls in a higher range of between 1.0% and 1.5%. Only three distinctive reflectance peaks were observed for G#5. A summary of the relative frequencies of the vitrinite reflectance classes in the distribution range of each coal is provided in Table 4.7.

Table 4.7 Vitrinite reflectance distributions for each coal.

Vitrinite reflectance distribution	*Unit*	*INY*	*UMZ*	*G#5*	*TSH*
Rr% Distribution					
V5	%	1.0		14.0	
V6	%	13.0	10.0	68.0	
V7	%	38.0	48.0	18.0	
V8	%	31.0	27.0		
V9	%	16.0	14.0		
V10	%	1.0	1.0		4.0
V11	%				44.0
V12	%				33.0
V13	%				6.0
V14	%				8.0
V15	%				3.0
V16	%				2.0
	%				
Mean Rr%	%	0.81	0.81	0.66	1.23
Standard deviation (σ) %	-	0.09	0.09	0.05	0.12
Range	%	0.5-1.0	0.5-1.0	0.5-0.7	1.0-1.6

Table 4.7 refers to the V-classes of vitrinite, where V5 to V10 indicate the reflectance distribution range of 0.5% to 1.0%. The extent of the distribution range of vitrinite reflectance for each coal sample is indicated by the calculated standard deviations. The standard deviations for the vitrinite-class distributions of coals INY, UMZ and G#5 were less than 0.1%, which is typical for single seam, non-blended coals as described in the terminology of the ECE-UN International Codification System for Medium and High Rank coals (Du Cann, 2010).

The standard deviation for the vitrinite-class distribution of the TSH sample was slightly higher with a value of 0.12%. This, with inclusion of the extended reflectance distribution in comparison to the other three coals, indicates that TSH could have encountered some thermal effects (Du Cann, 2010). The latter does, however, not exclude the fact that sample heterogeneity could also have affected the vitrinite-class distribution of the TSH sample. Furthermore, the vitrinite random reflectance values (used in rank classification) were calculated respectively as 0.66%, 0.81%, 0.81% and 1.23% for coals G#5, INY, UMZ and TSH. From the vitrinite random reflectance data, these four samples are classified as bituminous Medium Rank C to B coals,

with coal TSH ranking the highest (ISO 11760-2005 standard) (ISO, 2005). Coal rank plays a very important role in devolatilization and can have a remarkable effect on the devolatilization behaviour of a particular coal as well as the product spectrum of tars, chars and gases generated (Iglesias *et al*., 2001; Smith *et al*., 1994; Solomon & Hamblen, 1985). Although differences occur in the vitrinite reflectance of each coal, all four coals are classified as Medium Rank Bituminous coal, thus in accordance with the goals of coal choice as set forth in Section 4.2. Due to the difference between the values of the vitrinite random reflectance of each coal, it is expected that the devolatilization behaviour of these coals will be quite different. For this particular case, when compared to the chemical properties of the coals, it can be seen that volatile matter content increases monotonically with a decrease in vitrinite reflectance (or rank). This excludes external limiting factors such as mineral composition and physical properties to just name a few.

Total maceral reflectance scans were also conducted on all four coal samples. These analyses involved taking 250 random reflectance readings on all of the organic constituents i.e.: vitrinites, liptinites and inertinites (Du Cann, 2010). The obtained reflectance histograms are provided in Figure 4.2, while the corresponding detailed results are presented in Table A.3 of Appendix A.3.

From Figure 4.2 it is evident that the characteristics of the four scans varied considerably. Maceral reflectance scans of coals UMZ and INY were quite similar, with only slight differences between certain reflectance ranges. This was, however, not true for the G#5 and TSH samples, which showed substantial differences amongst each other, with coal G#5 showing a significant peak of nearly 30% relative frequency at a reflectance of 0.6% (Du Cann, 2010).

The results obtained from maceral reflectance were further used to determine the mean random scan values and the total reactives (m.m.f.b.) of each coal sample. The calculated mean random scan values ranged between 0.96% and 1.46% and decreased in the order from TSH > UMZ > INY > G#5. In comparison, coals G#5 and TSH exhibited similar amounts of total reactives with values of 73% and 74% (m.m.f.b.), respectively. There was however some difference between the values for coals INY and UMZ, with coal INY constituting about 60% of total reactives, whilst the amount of reactives for coal UMZ differed by 8%, i.e.: 52%.

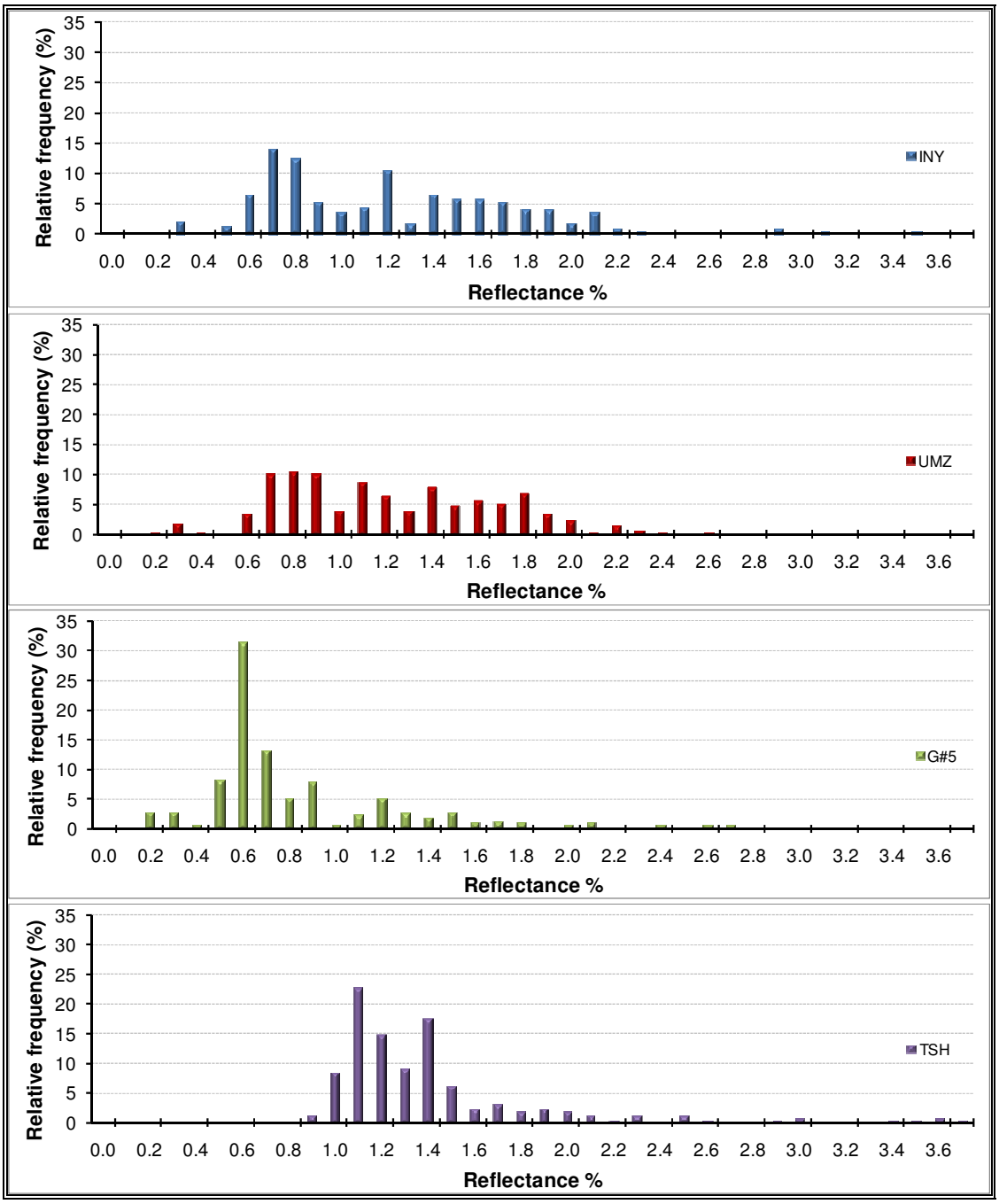

Figure 4.2 Total maceral reflectance scan histograms for the four coals.

A brief summary of the important results as obtained from maceral scan analyses is summarised in Table 4.8. The standard deviation again gives an indication of the extent of the distribution range (Du Cann, 2010).

Table 4.8 Summary of maceral scan analyses.

Coal sample	*Random Scan Values*	*Reflectance Distribution*	*σ*	*Total reactives from scan*
INY	1.26%	V3 to V35	0.527	60%, m.m.f.b.
UMZ	1.27%	V2 to V26	0.467	52%, m.m.f.b.
G#5	0.96%	V1 to V32	0.571	73%, m.m.f.b.
TSH	1.46%	V9 to V37	0.475	74%, m.m.f.b.

Organic composition:

Organic (maceral) composition and mineral content (vol.%) (from a petrographic point of view) was determined with point count analysis. The results obtained from this technique are summarised in Table 4.9, whereas a full description of the different maceral distributions is provided in Table 4.10.

Table 4.9 Summary from point count analyses.

	% by Volume (m.m.b.)			
Coal sample	*Total Vitrinite*	*Total Liptinite*	*Total Inertinite*	*Visible Minerals*
INY	33	3	54	10
UMZ	22	3	65	10
G#5	56	9	28	7
TSH	63	1	27	9

From the point count analysis it is evident that all four coals displayed a marked variation in organic composition. Two of the coals, INY and UMZ, were found to be inertinite-rich (54 vol.% and 65 vol.%, m.m.b., respectively), whilst coal G#5 and TSH contained significantly larger amounts of vitrinite (56 vol.% and 63 vol.%, m.m.b., respectively), which is typical for the Witbank No. 2, 4 and 5 seams; and the Venda-Pafuri coalfield (Pinheiro, 1999). The vitrinite content of TSH was, however, lower than that reported by Pinheiro (1999), due to the fact that the sample used was a float fraction at -1.5 $g.cm^{-3}$, whilst the reported value is for the final beneficiated plant product (which is dense medium separated at -1.4 $g.cm^{-3}$).

Table 4.10 Organic (Maceral) composition of the four coals.

MACERAL ANALYSES (% BY VOLUME, MINERAL MATTER BASIS)															
	Vitrinite			*Liptinite*			*Inertinite*							*Visible Minerals %*	*Total Reactives %*
Coal	*VIT %*	*PV %*	*TV %*	*S/R/C %*	*ALG %*	*TL %*	*RSF %*	*ISF %*	*F/ SEC %*	*MIC %*	*R INT %*	*I INT %*	*TI %*		
INY	32	1	***33***	3	0	***3***	11	20	4	1	6	12	***54***	***10***	***53***
UMZ	22	0	***22***	3	0	***3***	16	24	5	2	5	13	***65***	***10***	***46***
G#5	55	1	***56***	9	0	***9***	6	10	3	1	2	6	***28***	***7***	***73***
TSH	60	3	***63***	1	0	***1***	5	8	6	>1	2	6	***27***	***9***	***71***

NOMENCLATURE:

VIT : Vitrinite
PV : Pseudo-vitrinite
TV : Total vitrinite
S/R/C : Sporinite/Resinite/Cutinite
ALG : Alginite
TL : Total liptinite

RSF : Reactive semifusinite
ISF : Inert semifusinite
F/SEC : Fusinite / Secretinite
MIC : Micrinite
R INT : Reactive Inertodetrinite
I INT : Inert Inertodetrinite

TI : Total inertinite
Total reactives = TV+TL+RSF+RINT

It is, however, known that the vitrinite for Medium rank bituminous coals such as INY, UMZ, G#5 and TSH devolatilize upon heating and tend to form porous carbon chars (Du Cann, 2010), whereas the inertinite macerals tend to form more dense, inert chars during devolatilization (Falcon & Snyman, 1986).

The variance in maceral content does, however, conform to the goal of sample choice that was set out in Section 4.2. The liptinite macerals of each coal accounted for between 1 vol.% (m.m.b.) and 9 vol.% (m.m.b.) of the total macerals and was mainly distributed among sporinite with some cutinite. Alginite was, however, only very rarely seen in all four samples. Coals INY and UMZ constituted large proportions of "tissue type" inertinites (fusinites and semifusinites) in comparison to the less abundant "detrital" inertodetrinites i.e.: micrinites, reactive inertodetrinites and inert inertodetrinites (Du Cann, 2010). In comparison to the other two associated macerals, the hydrogen-rich liptinite maceral produces the highest amount of volatile matter upon heating (Cloke & Lester, 1994; Du Cann, 2010, Tsai, 1982). This is also clear from the chemical analyses, where volatile matter content increases with increasing liptinite content as can be seen in Figure 4.3a.

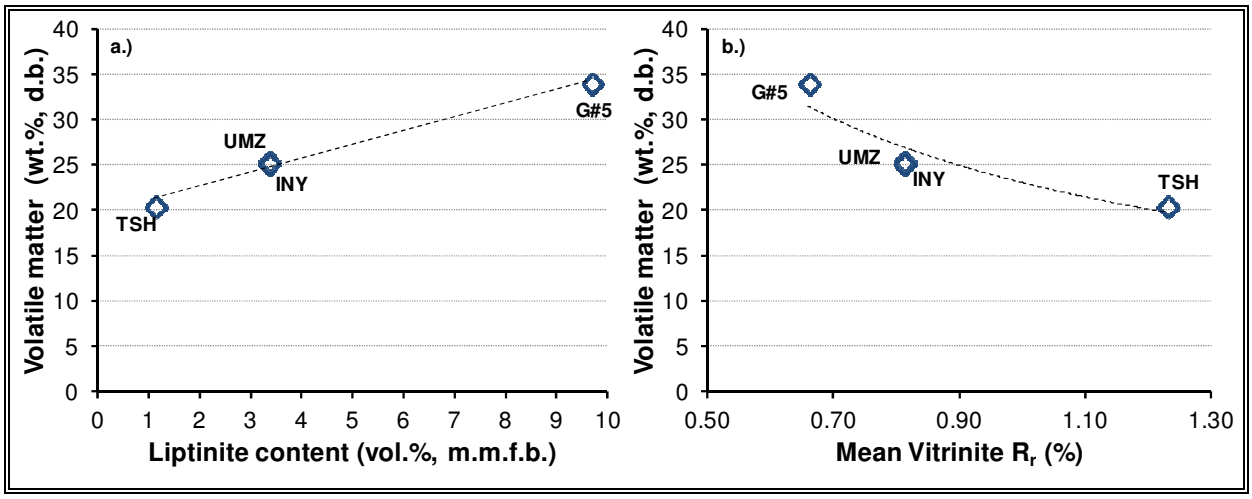

Figure 4.3 Comparison of volatile matter content with a.) liptinite content and b.) rank.

A comparison between the volatile matter content and mean vitrinite reflectance (Mean R_r%) of each coal (Figure 4.3b) does however provide evidence of the well-known rank dependent effect of volatile matter content as supported by the findings of Borrego *et al*. (2000). The higher volatile matter content of G#5 can therefore be ascribed to both its substantially larger liptinite content of 9 vol.% (m.m.b.) and lower rank (Mean Rr% of 0.66%) in comparison to the other

three coals. From a mineral perspective, visible minerals accounted for 10 vol.% (m.m.b.) or less for all the coals, with coals INY and UMZ containing the highest amounts of these species (Du Cann, 2010). This is in agreement with what was found from the proximate analysis. Although liptinite is more susceptible during heating, it does not solely constitute the whole volatile matter content of a coal. In order to evaluate the contribution of each maceral to the volatile matter of the four coals, a prediction method as developed by Borrego *et al*. (2000) was followed. According to Borrego *et al*. (2000) the volatile matter content of a coal can be predicted from its maceral content by the following equation:

$$VM = \sum_{j}^{n} \phi_j Y_j; \quad n = \textit{inertinite, vitrinite and liptinite} \qquad \text{Equation (4.1)}$$

Where ϕ_j represents the fractional volatile matter content of maceral *j* and Y_j is the content of maceral *j* (m.m.f.b.) in the coal. The fraction of volatile matter content of each coal maceral can be determined from empirical correlations derived from experiments conducted by Borrego *et al*. (2000) on 39 selected coals with varying rank and maceral composition. These correlations are functions of fitting parameters and the vitrinite random reflectance of a coal as defined in Table 4.11.

Table 4.11 Estimation of VM from maceral content (Borrego *et al*., 2000).

Maceral	***Random vitrinite Reflectance Range (R_r %)***	***Expression for ϕ_j***	***Fitting parameters***
Vitrinite	0.42 – 6.08%	$\frac{v_1}{R_r^{0.5} - R_r^{0.333} - v_4} + v_5$ Equation (4.2)	$v_1 = 1.726; \quad v_2 = 3.984;$ $v_3 = -0.670; \quad v_4 = -5.837;$ $v_5 = 0.051$
Inertinite	0.42 – 6.08%	$i_1 \cdot \exp\left[-\left(\frac{R_r}{i_2}\right)^{i_3}\right]$ Equation (4.3)	$i_1 = 0.325;$ $i_2 = 2.642;$ $i_3 = 0.883$
Liptinite	0.42 – 6.08%	$\frac{l_1 + R_r^{l_2}}{R_r^{l_3} - R_r^{l_4} - l_5} + l_6$ Equation (4.4)	$l_1 = -0.508; \quad l_2 = 0.735;$ $l_3 = 5.333; \quad l_4 = -0.496;$ $l_5 = -1.560; \quad l_6 = 0.132$

Furthermore the volatile matter contribution of each maceral can be estimated by Equation (4.5) (Borrego *et al*., 2000):

$$VM_j = VM - \sum_{m \neq j} \phi_m Y_m \qquad \text{Equation (4.5)}$$

With VM_j the volatile matter contribution from maceral *j* and the subscript *m* pertaining to the other two residual macerals. From this the percentage contribution of each maceral (ζ_i) can be calculated as:

$$\zeta_j = \frac{VM_j}{VM} \qquad \text{Equation (4.6)}$$

The values as obtained from Equations 4.1-4.6 are summarised in Table 4.12.

Table 4.12 Volatile prediction parameters for the coals.

VOLATILE MATTER PREDICTION					
Parameter	***Unit***	***INY***	***UMZ***	***G#5***	***TSH***
$\phi_{vitrinite}$	-	0.39	0.39	0.42	0.29
$\phi_{liptinite}$	-	0.58	0.58	0.65	0.31
$\phi_{inertinite}$	-	0.23	0.23	0.24	0.20
$VM_{Predicted}$	***wt.% (m.m.f.b)***	***29.9***	***27.9***	***38.7***	***26.1***
$\zeta_{vitrinite}$	%	47.6	34.0	64.9	76.5
$\zeta_{liptinite}$	%	6.5	6.9	16.3	1.3
$\zeta_{inertinite}$	%	45.9	59.1	18.8	22.2

From Table 4.12 it is again clear that the liptinite content of coal G#5 contributes significantly to the volatile matter of the coal, with a theoretical contribution of about 16.3%. In contrast, however, almost 80% of the volatile matter of coal TSH can be attributed to its vitrinite content. The predicted volatile matter (m.m.f.b.) of each coal correlates very well with the experimental volatile matter contents (d.a.f.) from the proximate analyses as can be seen from Figure 4.4.

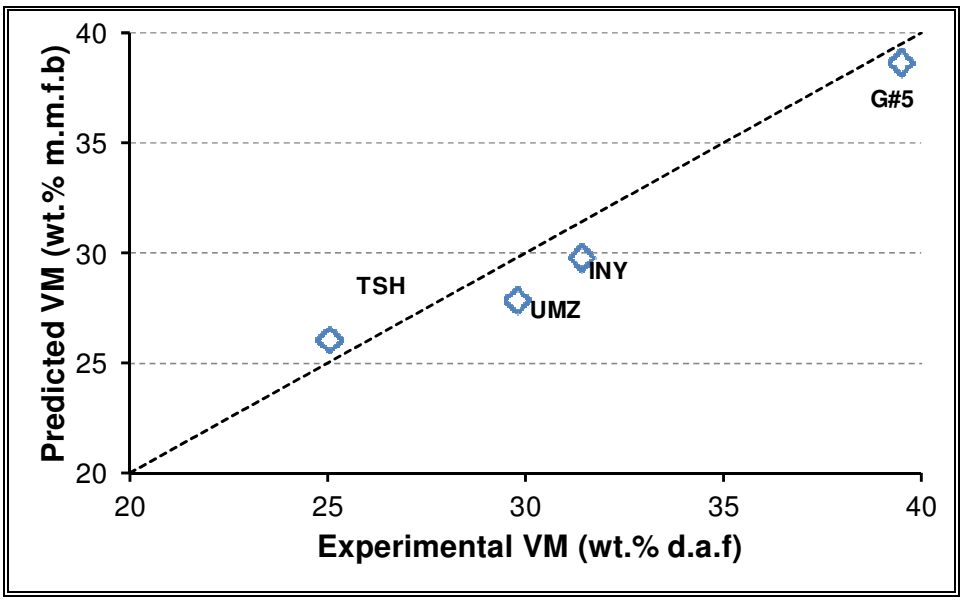

Figure 4.4 Parity plot of predicted VM against experimental VM.

For the purpose of petrographic composition, maceral reactivity is defined as the propensity of the different macerals of coals to react upon heating (Du Cann, 2010). Although vitrinite and liptinite are generally accepted to be the reactive organic constituents, there are, however, certain inertinite group macerals that tend to behave in a similar manner (Cloke & Lester, 1994; Du Cann, 2010). These reactive inertinites are normally classified as reactive inertodetrinites and reactive semifusinites; and form part of another petrographic parameter defined as the total reactive macerals:

$$Total\ reactive\ macerals = TV + TL + RSF + RINT \qquad \text{Equation (4.7)}$$

As in the case for the total maceral reflectance scan, coal G#5 and TSH contained the largest amount of reactive macerals (73 vol.% and 71 vol.% respectively). With consideration of both chemical- (Section 4.6.1.1) and petrographical analyses it is evident that the amount of volatiles is not governed by the amount of reactives. Although coal TSH contains the second largest amount of reactive macerals, it has the smallest amount of volatile matter. There seems however to be some correlation with the tar yield from Fischer tar analysis and the amount of reactive macerals. The amount of tar increases with an increase in reactive macerals. Again, this does not explain the relative contribution of each reactive maceral to the tar yield, nor does it specify the molecular structure of the species contained in the tars.

In an attempt to describe the yield of tar from a Fischer-assay, the combination of the effect of macerals into one descriptive parameter was sought. One such index, defined as the Maceral index (*MI*), was developed by Su *et al*. (2001) to predict the effect of maceral content and rank on the ignition and burn-out behaviour of coals (Hattingh, 2009; Su *et al*., 2001). The derivation of this parameter was based on the fact that (Su *et al*., 2001): (1) liptinite burns out rapidly due to its high volatile content, (2) the burn-out behaviour of vitrinite is mainly dependent on its reflectance, while inertinite burns out more difficultly and (3) the burn-out behaviour is dependent on the heating value of the specific coal under consideration. The *MI* can therefore be expressed as:

$$MI = (HVF)^{2.5} \cdot RF \qquad \text{Equation (4.8)}$$

Where;

$$HVF = \frac{HV}{30} \qquad \text{Equation (4.9)}$$

And;

$$RF = \frac{LIP + \left(VIT / R_r^2 \right)}{INT^{1.25}} \qquad \text{Equation (4.10)}$$

In the above equations, *HVF* refers to the heating value factor, *RF* the reactivity factor, *LIP* to the total liptinite content (m.m.f.b.), *VIT* to the total vitrinite content (m.m.f.b.), *INT* to the total inertinite content (m.m.f.b.) and *HV* to the heating value (d.b.) of the coal. A plot of Fischer tar yield against *MI* reveals a distinct correlation between the two quantities, which is illustrated in Figure 4.5. Fischer tar yield increases with increasing *MI*, with coals TSH and G#5 exhibiting the higher *MI* values due to increased levels of vitrinite as well as a high amount of liptinite in particular for coal G#5. The *INT* quantity in Equation (4.10) can, however, be substituted with a parameter defined as the *INR*, which allows for the non-reactive inertinite macerals. The difference between these two parameters is that *INR* originates from subtracting the semifusinite (reactive and non-reactive) content from the original *INT* parameter. This is done to exclude the high reactivity of this component (Helle *et al*., 2003).

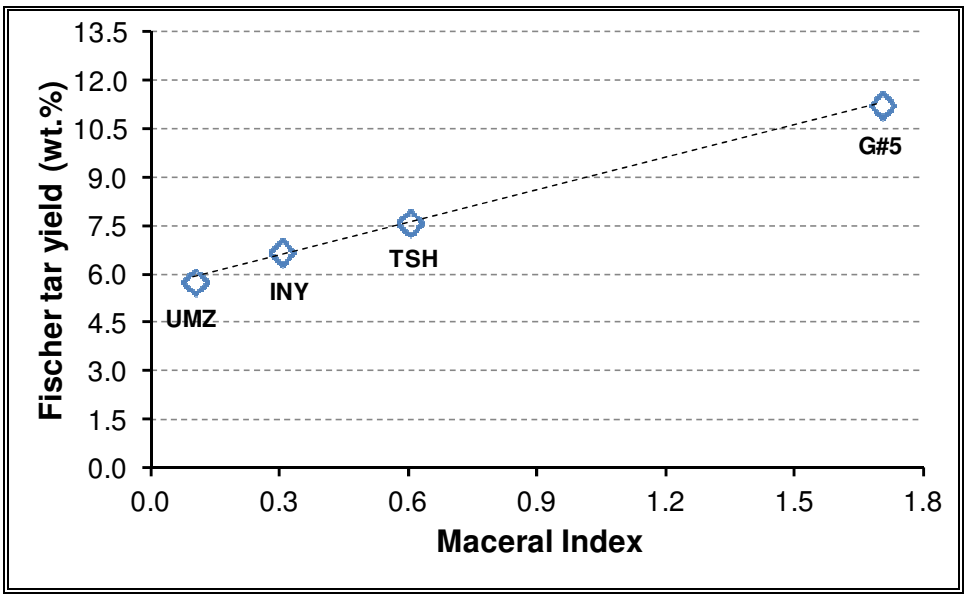

Figure 4.5 Comparison between Maceral Index and Fischer tar yield.

For this particular case the *MI* is referred to as the reactive maceral index (*RMI*). Evaluating this quantity with regard to Fischer tar yield produces similar results as observed in Figure 4.6.

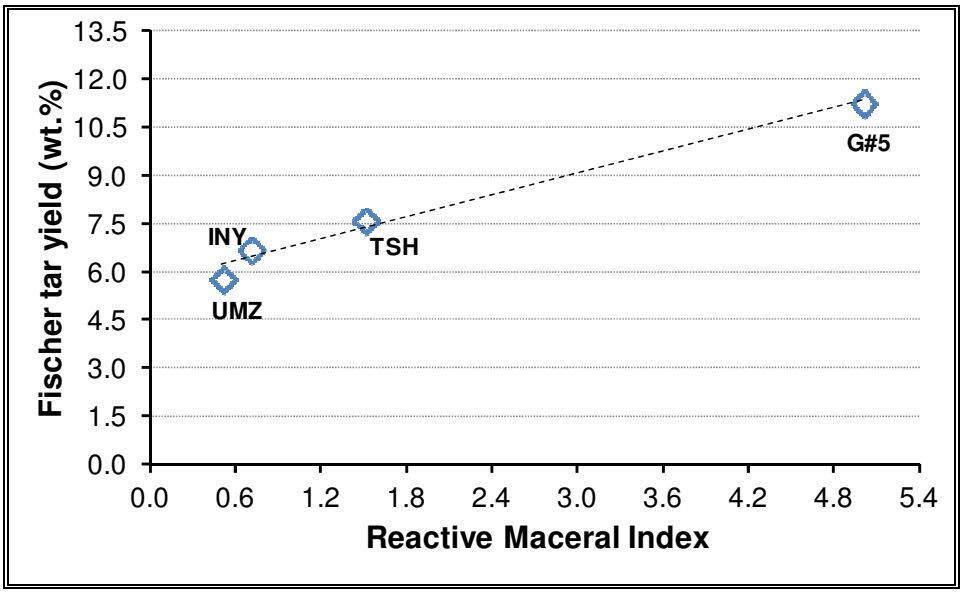

Figure 4.6 Comparison between Reactive maceral index and Fischer tar yield.

This indicates that with the exclusion of the semifusinites no change in the order of tar yields can be observed, thus proposing that the amount of highly reactive macerals (vitrinite and liptinite) possibly dictates the formation of tar. At this stage the same can, however, not be said for the molecular structure of the entities contained in the tar.

Microlithotype analyses:

The distributions of microlithotypes within each of the four coal samples are presented in Table 4.13. From the results it is clear that none of the four samples contained any liptinite in its “pure” form (liptite). A substantial difference was, however, observed between the amounts of vitrite and inertite contained in each coal. Coal TSH was vitrite dominant (45 vol.%, m.m.b.), with a relatively low amount of inertite (14 vol.%, m.m.b.). In contrast, coals INY and UMZ contained a correspondingly higher amount of inertite (33 vol.%, m.m.b.), with lower vitrite contents amounting to 19 vol.% (m.m.b.) and 7 vol.% (m.m.b.), respectively. Of all four coals, G#5 constituted the lowest concentration of the monomaceral, inertite, with a value of 10 vol.% (m.m.b.).

The intermediate (bi- and tri-macerals) maceral-maceral associations reported values of well over 30 vol.% (m.m.b.) for all four coals, with coal INY containing the smallest amount of these species. No significantly large variances were observed between the bi-maceral contents of the four coals, with the exception of coals UMZ and G#5, which contained the largest amount of durite (16 vol.%, m.m.b.) and clarite (7 vol.%, m.m.b.), respectively in comparison to the other coals.

Tri-macerite composition varied between 1 vol.% (m.m.b.) and 28 vol.% (m.m.b.) and increased in the order: TSH < INY < UMZ < G#5. Throughout the whole range of coals, maceral/mineral associations (carbominerite) accounted for between 8 vol.% (m.m.b.) and 15 vol.% (m.m.b.). Mineral-rich particles reported in all cases did not exceed a value of 6 vol.% (m.m.b.).

It is, however, evident that coal TSH contained a larger amount of carbominerite (15 vol.%, m.m.b.) with respect to its minerite content (2 vol.%, m.m.b.), indicating that most of the inorganic species are contained within the carbon-matrix of the coal.

Table 4.13 Microlithotype composition of the four coals.

MICROLITHOTYPE ANALYSES (% BY VOLUME, MINERAL MATTER BASIS)											
	"Pure" monomacerals				*Intermediates*					*Carbominerite %*	*Minerite %*
					Bi-macerals			*Tri-macerals*	*TOTAL %*		
Coal	*Vitrite %*	*Liptite %*	*Inertite %*	*TOTAL %*	*Clarite %*	*Durite %*	*Vitrinertite %*	*Tri-macerite %*			
INY	19	0	33	***52***	1	5	17	9	***32***	10	6
UMZ	7	0	33	***40***	1	16	16	14	***47***	9	4
G#5	28	0	10	***38***	7	2	14	28	***51***	8	3
TSH	45	0	14	***59***	1	0	22	1	***24***	15	2

NOMENCLATURE:

Vitrite : Vitrinite > 95%
Liptite : Liptinite > 95%
Inertite : Inertinite > 95%
Clarite : Vitrinite + Liptinite > 95%
Durite : Inertinite+ Liptinite > 95%
Vitrinertite : Vitrinite + Inertinite > 95%
Tri-macerite : Vitrinite, Inertinite, Liptinite > 5%
Carbominerite : Total inorganic-organic microlithotypes
Minerite : > 60 vol.% minerals

Carbominerite- and minerite analyses:

Table 4.14 includes the results obtained from the carbominerite- and minerite analyses. The concentrations of the different carbominerite- and minerite species are expressed as a percentage of the total amount of carbominerite- and minerite, respectively.

Table 4.14 Carbominerite- and minerite species as a % of total carbominerite and minerite.

	CARBOMINERITE (%)		
Coal	***Carb-Argilite & Carbo-Silicate***	***Carbo-Pyrite***	***Carb-Ankerite***
INY	80.0	10.0	10.0
UMZ	66.7	11.1	22.2
G#5	75.0	12.5	12.5
TSH	86.7	6.7	6.7
	MINERITE (%)		
Coal	***Clay & Quartz Groups***	***Pyrite***	***Carbonate Group***
INY	50.0	16.7	33.3
UMZ	50.0	25.0	25.0
G#5	57.1	< 14.3	28.6
TSH	66.7	< 16.7	< 16.7

NOMENCLATURE:

Carb-Argilite : Coal + 20 to 60 vol.% clay minerals.
Carbo-Silicate : Coal + 20 to 60 vol.% quartz
Carbo-Pyrite : Coal + 5 to 20 vol.% sulphides
Carb-Ankerite : Coal + 20 to 60 vol.% carbonates

From Table 4.14 it can be seen that the carb-argilite and carbo-silicate groups are most commonly observed within all four samples. A larger amount of carb-ankerite was, however, observed for coal UMZ, suggesting that this coal contains more maceral-carbonate associations

with respect to the other three coals. In addition, the clay and quartz groups were the most frequently observed and was intimately associated with the macerals (Du Cann, 2010).

Pyrite concentrations of coals G#5 and TSH were found to be less than 1 vol.% (m.m.b). This was also true for the carbonate group concentration of coal TSH. The specific values were not obtained and for illustrative purposes a value of 0.5 vol.% (m.m.b.) was assumed to calculate the relative percentages in Table 4.14. It should however be added that for negligible amounts of pyrite in G#5 and TSH; and carbonate in TSH, the other tabulated values will be evidently higher. The main conclusion therefore should be that coal TSH contains insubstantially small amounts (irrespective of the exact values) of pyrite and carbonate groups as pure minerals.

General condition of the samples:

From the petrographic evaluation of the four coal samples it was observed that some of the particles displayed extensive cracks and micro-fissures (Du Cann, 2010). This can, however, be attributed to coal handling and -preparation. Therefore some of the cracking could be due to the somewhat brittle nature of coals containing this level of maturity of vitrinite.

The pyrite present in all samples was observed as a “fresh” bright yellow colour and obvious signs of severe weathering only occurred occasionally. Slight heating effects were, however, observed for the TSH sample (particles of elevated reflectance levels were occasionally observed) (Du Cann, 2010).

4.6.1.3 Physical analyses

Mercury porosimetry

Mercury porosimetry is a valuable technique for determining physical coal properties such as particle density, skeletal density and macroporous structure (total porosity, macropore volume etc.) (Debelak & Schrodt, 1979; Gürdal & Yalçin, 2001; Mahajan & Walker, 1978; Toda & Toyoda, 1972; Unsworth *et al.*, 1989; Walker *et al.*, 1988). Particles in the range of 10 mm were used to assess these properties, and the results obtained are provided in Table 4.15.

Table 4.15 Mercury porosimetry results of the four coals.

Physical property	*INY*		*UMZ*		*G#5*		*TSH*	
	Value	*Error %*	*Value*	*Error %*	*Value*	*Error %*	*Value*	*Error %*
Pore area ($m^2.g^{-1}$)	24.9	14.6	24.3	1.8	34.3	12.5	18.9	2.8
Median pore diameter (Å)	4.7	2.0	4.8	2.6	4.7	1.1	4.7	0.00
Average pore diameter (Å)	12.8	7.4	9.1	8.5	8.7	5.8	18.2	10.7
Particle density ($kg.m^{-3}$)	1442	2.4	1460	2.8	1333	4.2	1368	3.0
Skeletal density ($kg.m^{-3}$)	1628	1.7	1588	3.7	1480	3.1	1551	3.3
Porosity (%)	11.4	15.1	8.1	9.7	9.9	12.8	11.8	7.8

From Table 4.15 it can be seen that coal TSH has the lowest pore area; but the highest average pore diameter and porosity in comparison to the other three coals. It should, however, be noted that the porosity provided in Table 4.15 is only measured over the macropore range ($1.9 \times 10^4 < d_{pore} < 174.7 \times 10^4$ Å), due to the fact that the intruded mercury cannot penetrate the micropores. Coal UMZ has the largest particle density, while coal INY has the largest skeletal density, which can be mainly attributed to either the higher amount of inertinite (more dense material) or the slightly larger amount of minerals present in these two coals. The particle density as determined through mercury intrusion forms an important part in the prediction of micro- and mesoporosity as evaluated through CO_2- and N_2 adsorption. The errors obtained from the mercury porosimetry are for some cases larger than 10%, but could be a direct consequence of the heterogeneity of large coal particles (10 mm).

CO_2- and N_2 adsorption analyses

In addition to mercury porosimetry, the low-temperature adsorption of gases such as CO_2 and N_2 can provide some valuable insight into the micro- and mesoporous structure of a particular coal (Hattingh, 2009). The use of CO_2 as adsorbent is normally confined to the determination of microporous properties, whereas N_2 adsorption measurements includes the mesopore range (Marsh, 1987; Gürdal & Yalçin, 2001; Sing *et al.*, 1985). The micropore range normally includes pore sizes smaller than 12 Å, while the mesopore- and macropore range extends from 12 Å to 300 Å and greater than 300 Å, respectively (Tsai, 1982). The isotherm data obtained from CO_2 adsorption analyses of the four coals is provided in Figure 4.7.

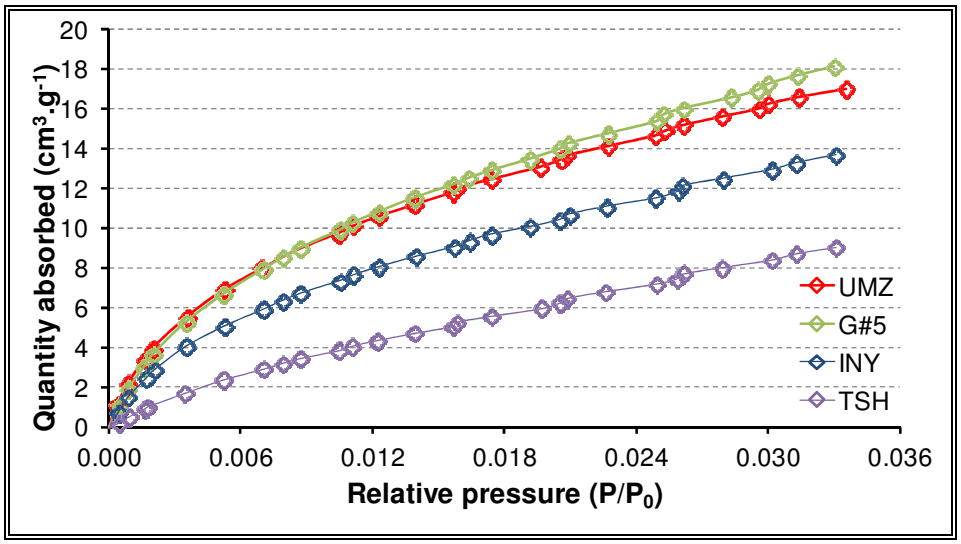

Figure 4.7 CO_2 adsorption isotherms for the four coals.

From this Figure it is evident that the isotherms of all four coals exhibit Type I behaviour, which is characteristic of microporous materials (Lowell *et al.*, 2004). The filling of micropores and the subsequent increased uptake of the adsorbent is normally associated with relatively low pressures (as seen in Figure 4.7), mainly due to the narrow pore width and high adsorption potential of micropores. In this particular case the accessible micropore volume is the governing mechanism for adsorbent uptake rather than the internal surface area (Lowell *et al.*, 2004). The structural parameters as obtained from CO_2 adsorption is summarised in Table 4.16. The Dubinin-Radushkevich (D-R) equation was applied accordingly to the isotherm data in order to determine the micropore surface area and monolayer capacity, respectively.

Table 4.16 CO_2 adsorption results of the four coals.

Physical property	*INY*	*UMZ*	*G#5*	*TSH*
Micropore Surface Area ($m^2.g^{-1}$)	119.5	140.6	153.2	87.6
Monolayer capacity ($cm^3.g^{-1}$)	26.2	30.8	33.5	19.2
Langmuir Surface Area ($m^2.g^{-1}$)	87.0	100.8	109.4	77.7
*Porosity for pores smaller than 5Å (%)	3.1	3.8	3.8	2.0
Average micropore diameter (Å)	4.1	3.9	4.0	4.3

**Calculated from the bulk densities determined with mercury intrusion.*

The isotherm data was also further used in assessing the Langmuir- and micropore surface areas (Dubinin-Radushkevich). As mentioned previously, micro-porosities were calculated with the use of the bulk density values as determined from mercury intrusion. The calculated values are displayed in Table 4.16 for all four coals (the calculation is discussed in Appendix A.4). The

error associated with determination of the different physical properties from CO_2 adsorption was found to be smaller than 4% for all cases. From the results it is evident that coal G#5 had the largest micropore surface area with a value of 153.2 $m^2.g^{-1}$. Coal TSH had the smallest micropore surface area, monolayer capacity and micro-porosity in comparison to the other three coals. Numerous authors (Castellò *et al.*, 2002; Debelak & Schrodt, 1979; Hurt *et al.*, 1991; Nandi & Walker, 1964) have established that the surface areas obtained from CO_2 adsorption are far larger in order than those obtained from N_2 adsorption. It is therefore proposed that the micropore surface area measured with CO_2 as adsorbent should give a much better prediction of the real reaction surface area available during coal conversion (Kajitani *et al.*, 2006).

An overview of the adsorption- and desorption isotherms as obtained from N_2 gas adsorption experiments is presented in Figure 4.8, while the important physical parameters determined from nitrogen adsorption is summarised in Table 4.17.

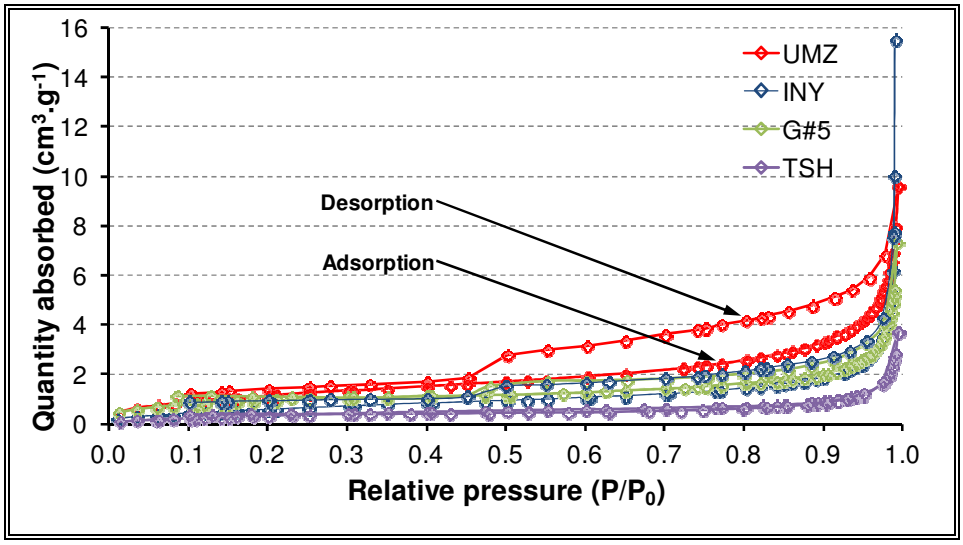

Figure 4.8 Nitrogen adsorption- and desorption isotherms for the four coals.

Both desorption- and adsorption isotherms were observed during analysis of the four coals. For all four coal samples, the adsorption isotherms exhibited plateau-like behaviour which is consistent with Type II isotherms as described by Brunauer *et al.* (1940), Gregg & Sing (1982) and Lowell *et al.* (2004). The combined isotherms of all four coals, however, displayed hysteresis behaviour and could therefore be characterised as Type IV isotherms (Brunauer *et al.*, 1940; Gregg & Sing, 1982). The presence of a hysteresis loop is normally associated with the occurrence of pore condensation (Lowell *et al.*, 2004). The formation of a plateau region can

be attributed to the limited uptake over a range of high relative pressure, which indicates complete pore filling. The inflection point or knee of the Type IV isotherms (which indicates the completion of monolayer coverage and the initiation of multilayer coverage) is consistent with what is typically observed for Type II isotherms (Lowell *et al*., 2004). The presence of Type IV isotherms indicates that apart from micropores, mesopores also form part of the coal-physical structure (Hattingh, 2009, Lowell *et al*., 2004).

Table 4.17 Nitrogen adsorption analysis results.

Physical property	*INY*	*UMZ*	*G#5*	*TSH*
Surface Area ($m^2.g^{-1}$):				
Single-point surface area at P/P_0 = 0.3	2.21	3.46	3.21	1.19
BET surface area	2.34	3.63	3.36	1.44
Langmuir Surface Area	3.72	5.59	4.98	2.10
t-plot External Surface Area	3.44	4.61	3.59	1.79
BJH Adsorption Surface Area of Pores (17Å<d_{pore}<3000Å)	2.34	3.05	2.04	1.05
BJH Desorption Surface Area of Pores (17Å<d_{pore}<3000Å)	3.26	5.77	3.27	0.98
Pore Volume ($cm^3.g^{-1}$):				
Single point adsorption total pore volume (d_{pore} < 1253.1 Å at P/P_0 = 0.984)	8.20E-03	9.27E-03	6.65E-03	3.89E-03
Single point desorption total pore volume (d_{pore} < 833.7 Å at P/P_0 = 0.976)	6.64E-03	1.00E-02	6.36E-03	2.74E-03
BJH Adsorption Volume of Pores (17Å<d_{pore}<3000Å)	2.36E-02	1.44E-02	1.05E-02	1.08E-02
BJH Desorption Volume of Pores (17Å<d_{pore}<3000Å)	2.40E-02	1.53E-02	1.16E-02	1.09E-02
Pore Size (Å):				
Adsorption average pore width	443.67	333.48	341.49	471.11
Desorption average pore width	359.56	361.10	326.63	331.33
BJH Adsorption Average Pore Diameter (17Å<d_{pore}<3000Å)	403.83	194.34	207.06	425.78
BJH Desorption Average Pore Diameter (17Å<d_{pore}<3000Å)	294.78	107.13	142.08	431.05
*Porosity (17Å<d_{pore}<3000Å) (%)	3.10	1.77	1.10	1.14

**Calculated from the bulk densities determined with mercury intrusion.*

The hysteresis behaviour of typical Type IV isotherms was less observable for coals G#5 and TSH and suggests that the isotherms of these two coals are more consistent with Type II isotherms. It is therefore evident that these two coals contain fewer mesopore structures in comparison to the two inertinite-rich coals. This observation is also reflected in the porosity

values obtained from N_2 adsorption. From Table 4.17 it is clear that the surface area (as determined from N_2 adsorption) of the four coals ranged between 0.98 $m^2.g^{-1}$ and 6.67 $m^2.g^{-1}$. In all four cases the BET surface area was less than the corresponding Langmuir- and t-plot external surface area. This could be ascribed to the fact that the linear relationship of the BET equation is only maintained for gas adsorption in a relative pressure range between 0.05 and 0.35 (Brunauer *et al.*, 1938). The average pore width (adsorption and desorption) of all four coals were found to be in the order expected for the mesopore range, with both coals G#5 and UMZ having the smallest average pore widths. The porosities from N_2 adsorption were determined in a similar manner as was done for CO_2 adsorption. A comparison between the porosities determined by the three different techniques is provided in Table 4.18.

Table 4.18 Comparison between porosities determined from different techniques.

% Porosities	*INY*	*UMZ*	*G#5*	*TSH*
Mercury porosimetry ($1.9 \times 10^4 < d_{pore} < 174.7 \times 10^4$ Å)	11.4	8.1	9.9	11.8
CO_2 adsorption ($d_{pore} < 5$ Å)	3.1	3.8	3.8	2.0
N_2 adsorption ($17 < d_{pore} < 1543$ Å)	3.1	1.8	1.1	1.1

From this Table it is evident that the porosity determined by mercury porosimetry is the largest for all three coals. This could be possibly attributed to the fact that a very large pore distribution range is measured during mercury porosimetry analyses. In addition, the N_2 adsorption porosity of coal INY was similar in value to CO_2 adsorption, indicating that this coal has the largest number of pores in the mesopore range in comparison to the other coals. Furthermore, the obtained CO_2- and N_2 adsorption results are in accordance with what was observed in previous studies (Hattingh, 2009; Koekemoer, 2009).

Coal plasticity and swelling behaviour

Three additional physical analyses, free swelling index (FSI), Gieseler fluidity and Ruhr dilatometry were conducted in order to assess the coking/swelling propensity of each coal during devolatilization. The results obtained from these three analyses are presented in Table 4.19, while Figure 4.9 provides a graphical overview of the obtained Gieseler fluidity and Ruhr dilatometry results.

Table 4.19 FSI, Gieseler fluidity and dilatation results obtained for all four coals.

Analyses	*Unit*	*Standard*	*INY*	*UMZ*	*G#5*	*TSH*
Free swelling index (FSI)	-	SABS ISO 501:2003	1.0	0.5	0.5	9.0
Gieseler fluidity		SANS 6072:2009				
Initial softening temperature	℃		N/A	N/A	420	417
Maximum fluid temperature	℃		N/A	N/A	429	466
Solidification temperature	℃		N/A	N/A	436	506
Maximum fluidity	ddpm		N/A	N/A	2	1512
Ruhr dilatation		ISO 10329:2009				
Softening temperature	℃		416	425	394	375
Temperature of maximum contraction	℃		500	500	500	435
Temperature of maximum dilatation	℃		N/A	N/A	N/A	473
Maximum contraction	%		7	6	18	24
Maximum dilatation	%		N/A	N/A	N/A	25

The free swelling index (FSI) is defined as the measure of the swelling propensity (increase in volume) of a coal when heated under specified conditions (Speight, 2005). From the Table it can be seen that coals INY, UMZ and G#5 have quite similar FSI values, with the exception of TSH, which has a significantly higher FSI of 9. According to Speight (2005), TSH can therefore be classified as a strongly coking/caking coal (FSI values > 4), whilst coals INY, UMZ and G#5 are only non-coking/caking. Caking/coking coals undergo a variety of physical changes during heating under an inert atmosphere which include: softening, melting, fusing, swelling and re-solidification (Speight, 2005). Temperatures at which some of these physical changes occur in the plastic range can be identified with the aid of Gieseler fluidity and/or dilatation measurements. Definitions of the different characteristic temperatures as measured from Gieseler fluidity has been described by Speight (2005). From the Table it is evident that only noticeable changes in plastic nature could be recorded for coal G#5, while significant changes could be observed for coal TSH over the whole temperature range as depicted in Figure 4.9. The plastic nature of coal G#5 was found to extend from 420℃ to 436℃, while a larger temperature range for plastic behaviour was observed for coal TSH. The initial softening temperature for coal TSH (417℃) was found to be slightly lower than that of coal G#5 (420℃), while re-solidification only occurred at approximately 506℃ for coal TSH. In addition, coal TSH

was characterised with the largest maximum fluidity (measured as dial divisions per minute or ddpm), which is in accordance with the expected swelling nature of this coal as established from FSI measurements.

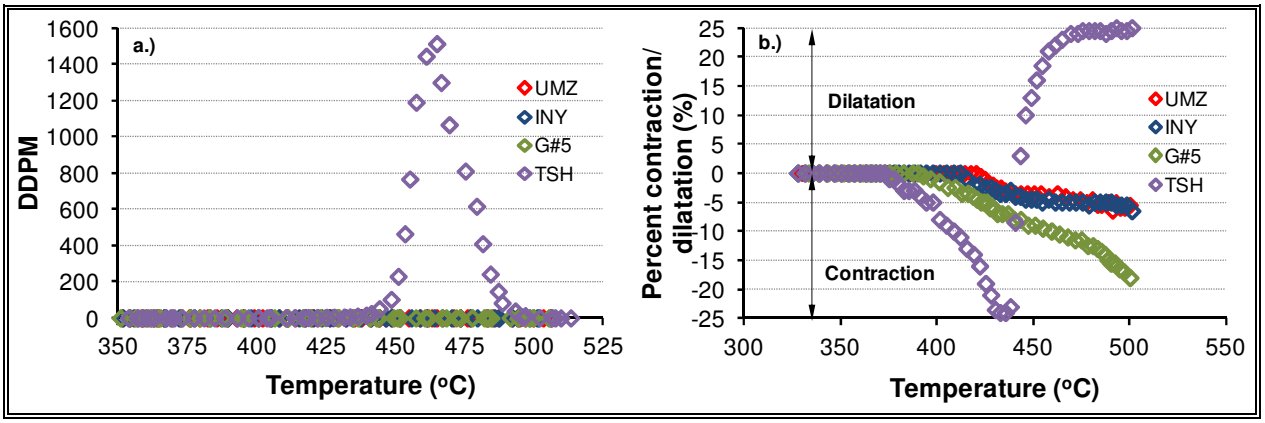

Figure 4.9 Graphical representations of results obtained from a.) Gieseler fluidity and b.) dilatometry tests performed on all four coals.

A comparison between dilatation results as presented in Table 4.19 and Figure 4.9 for the different coals showed remarkable differences, with only coal TSH displaying both significant levels of contraction (~24%) and dilatation (~25%). This provides supportive evidence that the devolatilization behaviour of coal TSH could have been characterised by a larger probability of metaplast formation. In contrast, however, only contraction was observed during the thermophysical behaviour of the other three coals. The degree of contraction (%) decreased in the order of TSH > G#5 > UMZ > INY, with similar behaviour exhibited by the two inertinite-rich coals. A maximum contraction temperature of 500°C (final temperature for dilatation test) was reported for coals INY, UMZ and G#5 due to the fact that no asymptotic value for contraction was observed by the end of the dilatation tests. Results for the different plasticity measurements from this investigation showed good agreement with findings made on other coals by Aoki *et al.* (2005), Speight (2005) and Yoshida et al. (2000).

4.7 Summary

All four samples were subjected to conventional characterization analyses, which revealed the respective chemical-, petrographical- and physical properties of each coal. From the proximate results it was evident that all four coals were found to contain relatively low ash yields (below 20 wt.%, d.b.), while volatile matter contents increased in the order TSH < UMZ < INY < G#5 and

were found to be well above 20 wt.% (d.b) for all four coals. Fischer-assays indicated that the largest amount of tar and gas could be obtained from coal G#5 (11.29 wt.% tar and 5.97 wt.% gas, respectively), while only a slightly higher tar yield (7.62 wt.%) was found for coal TSH in comparison to coals UMZ and INY (5.80 wt.% and 6.69 wt.%, respectively). From XRD and XRF it was evident that kaolinite, calcite, dolomite and pyrite were the predominant minerals present within the carbon structures of coals UMZ and INY, while kaolinite and quartz showed the highest abundance in the other two coals.

From a petrographical viewpoint, coals UMZ and INY were both characterised as inertinite-rich coals with inertinite contents of 72.2 vol.% (m.m.b.) and 60.0 wt.% (m.m.b.), respectively. In contrast, coals G#5 and TSH were found to contain substantial amounts of vitrinite (59.1 vol.% m.m.b. and 65.9 vol.% m.m.b., respectively), while a significant amount of liptinite (close to 10 vol.% m.m.b.) was additionally detected in the organic structure of coal G#5. Vitrinite reflectance measurements performed on the different samples indicated that all four coals were classified within the bituminous Medium B to C rank, with the highest vitrinite maturity associated with coal TSH. In addition, inert inertinite macerals (inert semifusinite and inert inertodetrinite) were found to dominate the inertinite maceral subgroup of each coal, which is in accordance with the petrographical nature of most South African coals.

Mercury porosimetry and gas adsorption (CO_2 and N_2) studies provided some additional insight into the physical structure of the different coals. True densities were found to range between 1333 kg/m^3 and 1460 kg/m^3, while total porosities (as determined from mercury porosimetry) varied between 8.1% and 11.8%. From CO_2 adsorption studies it was evident that all four coals contained substantial amounts of microporous structures of which the surface area ranged between 87.6 m^2/g and 153.2 m^2/g. Coal thermoplasticity- and swelling measurements (FSI, Gieseler fluidity and Ruhr dilatometry) confirmed the high coking/caking nature of coal TSH, while coals originating from the Witbank region (UMZ, INY and G#5) were found to only display contractive behaviour upon heating under an inert atmosphere.

Bibliography

ASTM (American Society for Testing and Materials). 1997. Standard test method for major and minor elements in coal and coke ash by X-ray fluorescence. Pennsylvania: ASTM International. (ASTM D4326).

Aoki, H., Miura, T., Itagaki, S. & Fukuda, K. 2005. Chapter 6: Analysis of dilatation and contraction of coal during carbonization. (*In* Komaki, I., Itagaki, S and Miura, T., *eds* Structure and thermoplasticity of coal. New York : Nova Science Publishers Inc. p. 109-117).

Bisset, H. 2005. Manufacture and optimization of tubular ceramic membrane supports. Potchefstroom: University of North-West. (Dissertation-M.Sc) 111 p.

Borrego, A.G., Marbán, G., Alonso, M.J.G., Álvarez, D. & Menéndez, R. 2000. Maceral effects in the determination of proximate volatiles in coals. *Energy & Fuels*, 14: 117-126.

Brunauer, S., Emmet, P.H. & Teller, E. 1938. Adsorption of gases in multimolecular layers. *Journal of the American Chemical Society,* 60(2): 309-319.

Brunauer, S., Deming, L.S., Deming, W.S. & Teller, E. 1940. On a theory of the Van der Waals adsorption of gases. *AIChE Journal*, 62:1723-1732.

Cairncross, B. 2001. An overview of the Permian (Karoo) coal deposits of southern Africa. *African Earth Sciences*, 33: 529-562.

Castelló, D.L., Amorós, D.C. & Solano, A.L. 2002. Can highly activated carbons be prepared with a homogeneous micropore size distribution. *Fuel Processing Technology*, 77-78: 325-330.

Cloke, M. & Lester, E. 1994. Characterization of coals for combustion using petrographic analysis: A review. *Fuel*, 73(3):315-320.

Debelak, K.A. & Schrodt, J.T. 1979. Comparison of pore structure in Kentucky coals by mercury penetration and carbon dioxide adsorption. *Fuel*, 58:732-736.

De Jager, G.E. 2002. Derivation of methodology capable of identifying suitable collectors for coal flotation by using surface dependant techniques. Cape Town: Cape Peninsula University of Technology. (Dissertation-M.Tech (Chemistry)) 146p.

Du Cann, V.M. 2010. A petrographic investigation of four bituminous coal samples. Test Report PSA 2010-159, Petrographics SA, Pretoria, South Africa. 9 p.

Exxaro. 2010. Annual Report for the year ended 31 December 2009. http://financialresults.co.za/2010/exxaro_ar2009/group_glance_operations.htm Date of access: 06 Dec. 2010.

Falcon, R.M.S. & Snyman, C.P. 1986. An introduction to coal petrography: Atlas of petrographic constituents in the bituminous coals of Southern Africa. Johannesburg : The Geological Society of South Africa. 106 p.

Furimsky, E. & Ripmeester, J. 1983. Characterization of Canadian coals by nuclear magnetic resonance spectroscopy. *Fuel Processing Technology,* 7(3): 191– 202.

Gürdal, G. & Yalçin, M.N. 2001. Pore volume and surface area of the Carboniferous coals from the Zonguldak basin (NW Turkey) and their variations with rank and maceral composition. *International Journal of Coal Geology*, 48:133-144.

Gregg, S.J. & Sing, K.S.W. 1982. Adsorption, surface area and porosity. 2nd Edition. London: Academic Press.

Hattingh, B.B. 2009. The determination of the reaction mechanisms involved in the CO_2 gasification of inertinite-rich, high ash coals. Potchefstroom: University of North-West. RSA. (Dissertation-M.Eng). 227p.

Hashimoto, K., Miura, K. & Ueda, T. 1986. Correlation of gasification rates of various coals measured by a rapid heating method in a steam atmosphere at relatively low temperatures. *Fuel*, 65:1516-1523.

Helle, S., Gordon, A., Alfaro, G., García, X. & Ulloa, C. 2003. Coal blend combustion: link between unburnt carbon in fly ashes and maceral composition. *Fuel Processing Technology* 80: 209-223.

Holdich, R.G. 2002. Fundamentals of particle technology. Leicestershire: Midland Information Technology and Publishing. p. 3-4.

Hurt, R.H., Sarofim, A.F. & Longwell, J.P. 1991. The role of microporous surface area in the gasification of chars from sub-bituminous coal. *Fuel*, 70: 1079-1082.

Iglesias, M.J., Cuesta, M.J. & Suraez-Ruiz, I. 2001. Structure of tars derived from low-temperature pyrolysis of pure vitrinites: Influences of rank and composition of vitrinites. *Journal of Analytical and Applied Pyrolysis*, 58-59: 255-284.

ISO (International Organization for Standardization). 1985. Methods for the petrographic analysis of bituminous coal and anthracite-Part 2: Preparation of coal samples. Geneva: ISO Standards. (ISO 7404-2).

ISO (International Organization for Standardization). 1994a. Methods for the petrographic analysis of bituminous coal and anthracite-Part 3: Method of determining maceral group composition. Geneva: ISO Standards. (ISO 7404-3).

ISO (International Organization for Standardization). 1988. Methods for the petrographic analysis of bituminous coal and anthracite-Part 4: Method of determining microlithotype-, carbominerite- and minerite composition. Geneva: ISO Standards. (ISO 7404-4).

ISO (International Organization for Standardization). 1994b. Methods for the petrographic analysis of bituminous coal and anthracite-Part 5: Method of determining microscopically the reflectance of vitrinite. Geneva: ISO Standards. (ISO 7404-5).

ISO (International Organization for Standardization). 2001. Solid mineral fuels - Determination of total carbon, hydrogen and nitrogen-instrumental methods. Geneva: ISO Standards. (ISO 12902).

ISO (International Organization for Standardization). 2005. Classification of coals. Geneva: ISO Standards. (ISO 11760).

ISO (International Organization for Standardization). 2006. Determination of total sulphur through IR spectroscopy. Geneva: ISO Standards. (ISO 19579).

ISO (International Organization for Standardization). 2009. Coal: determination of plastic properties: Gieseler plastometer method. Geneva: ISO Standards. (ISO 10329).

Jeffrey, L.S. 2005. Characterisation of the coal resources of South Africa. *The Journal of the South African Institute of Mining and Metallurgy,* 95-102.

Kajitani, S., Suzuki, N., Ashizawa, M. & Hara, S. 2006. CO_2 gasification rate analysis of coal char in entrained flow coal gasifier. *Fuel*, 85:163-169.

Koekemoer, A.F. 2009. The influence of minerals content and petrographic composition on the gasification of inertinite-rich, high ash coal. Potchefstroom: University of North-West. RSA. (Dissertation – M.Eng). 180p.

Lowell, S., Shields, J.E., Thomas, M.A. & Thommes, T. 2004. Characterisation of porous solids and powders: Surface area, pore size and density. Dordrect: Kluwer Academic Publishers. 353 p.

Mahajan, O.P. & Walker, P.L. 1978. Porosity of coals and coal products. DOE Tech. Rep. FE2030-TR7, 51 p.

Marsh, H. 1987. Adsorption methods to study microporosity in coals and carbons-a critique. *Carbon*, 25:49-58.

Milne, C. 2004. Scantech goes global with world-class analyzers. [Web:] http://scantech.com.au. [Date of use: 13 Jan. 2010].

Nandi, S.P. AND Walker, P.L. 1964. The diffusion of nitrogen and carbon dioxide from coals of various rank. *Fuel*, 43: 385-393.

Pinheiro, H.J. 1999. A techno-economic and historical review of the South African coal industry in the 19th and 20th centuries AND analyses of coal product samples of South African collieries 1998-1999. (In Bulletin 113. SABS: Pretoria. 97p.)

SANS (South African National Standard). 1984. Yields of tar, water, gas, and coke residue from coal by low temperature distillation. Pretoria: SABS, Standards Division. (SANS 6073).

SANS (South African National Standard). 1995. Determination of gross calorific value by the bomb calorimetric method, and calculation of net calorific value. Pretoria: SABS, Standards Division. (SABS ISO 1928).

SANS (South African National Standard). 1997. Solid mineral fuels: Determination of ash content. Pretoria: SABS, Standards Division. (SABS ISO 1171).

SANS (South African National Standard). 1998. Hard coal and coke: Determination of volatile matter. (SABS ISO 562).

SANS (South African National Standard). 2003. Hard coal - Determination of the crucible swelling number. Pretoria: SABS, Standards Division. (SABS ISO 501).

SANS (South African National Standard). 2007. Moisture content of coal samples intended for general analysis (air-oven method). Pretoria: SABS, Standards Division. (SANS 5925).

SANS (South African National Standard). 2009. Coking properties of coal (Ruhr dilatometer test). Pretoria: SABS, Standards Division. (SANS 6072).

Sing, K.S.W., Everett, D.H., Haul, R.A.W., Moscou, L., Pierotti, R.A., Rouquerol, J. & Siemieniewska, T. 1985. Reporting physisorption data for gas/solid systems; with special reference to the determination of surface area and porosity. *Pure applied chemistry*, 57:603-619.

Smith, W.H., Roux, H.J. & Steyn, J.G.H. 1983. The classification of coal macerals and their relation to certain chemical and physical parameters of coal. *Special publication of Geological Society of South Africa*. 7:111-115.

Smith, D.A.M. & Whittaker, R.L.G. 1986. The Springs-Witbank Coalfield. Anhaeusser, C.R. and Maske, S. (eds.). Mineral Deposits of Southern Africa. vol. II. Geol. Soc. S. Afr., Johannesburg, pp. 1969–1984.

Smith, K.L., Smoot, L.D., Fletcher, T.H. & Pugmire, R.J. 1994. The structure and reaction processes of coal. New York: Plenum Press. 473p.

Solomon, P.R. & Hamblen, D.G. 1985. Chapter 5: Pyrolysis in R.H. Schlossberg ed *Chemistry of coal conversion*, New York : Plenum Press. p. 121-251.

Spears, D.A. 2000. Role of clay minerals in UK coal combustion. *Applied Clay Science*, 16: 87-95.

Speight, J.G. 2005. Handbook of coal analysis. Vol. 166. USA: John Wiley & Sons Ltd. 238p.

Stanley-Wood, N.G. & Lines, R.W. 1992. Particle size analysis. Royal society of Chemistry. University of Technology. Loughborough, UK.

Su, S., Pohl, J.H. Holcombe, D. & Hart, J.A. 2001. A proposed maceral index to predict combustion behaviour of coal. *Fuel*, 80:699-706.

Thomas, L. 2002. Coal geology. England: John Wiley & Sons Ltd. 367 p.

Toda, Y. & Toyoda, S. 1972. Application of mercury porosimetry to coal. *Fuel,* 51:199-201.

Tsai, S.C. 1982. Coal science and technology 2: Fundamentals of coal beneficiation and utilization. Amsterdam: Elsevier Scientific Publishing company. 375p.

Unsworth, J.F., Fowler, C.S. & Jones, L.F. 1989. Moisture in coal: 2. Maceral effects on pore structure. *Fuel*, 68:18-26.

Verryn, S. 2010. Qualitative- and quantitative XRD analysis of four coal samples. Test Report, XRD Analytical & Consulting, Pretoria, South Africa. 3 p.

Walker, P.L., Verma, S.K., Utrilla, J.R. & Davis, A. 1988. Densities, porosities and surface areas of coal macerals as measured by their interaction with gases, vapours and liquids. *Fuel*, 67:1615-1623.

Yoshida, T., Iino, M., Takanohashi, T. & Katoh, K. 2000. Study on thermoplasticity of coals by dynamic viscoelastic measurement: effect of coal rank and comparison with Gieseler fluidity. *Fuel*, 79: 399-404.